Journal of Molecular Liquids 339 (2021) 116969

Contents lists available at ScienceDirect

Journal of Molecular Liquids

journal homepage: www.elsevier.com/locate/molliq

On the photophysical properties of a liquid crystal dimer based on 4-nitrostilbene: A combined experimental and theoretical study

Kristina Gak Simić [a], Ivana Đorđević [b], Goran Janjić [b], Dániel Datz [c], Tibor Tóth-Katona [c], Nemanja Trišović [d,*]

[a] Innovation Centre of the Faculty of Technology and Metallurgy, Karnegijeva 4, 11120 Belgrade, Serbia
[b] University of Belgrade - Institute of Chemistry, Technology and Metallurgy, National Institute of the Republic of Serbia, Njegoševa 12, 11001 Belgrade, Serbia
[c] Institute for Solid State Physics and Optics, Wigner Research Centre for Physics, P.O. Box 49, Budapest H-1525, Hungary
[d] Faculty of Technology and Metallurgy, University of Belgrade, Karnegijeva 4, 11120 Belgrade, Serbia

ARTICLE INFO

Article history:
Received 28 April 2021
Revised 16 June 2021
Accepted 8 July 2021
Available online 13 July 2021

Keywords:
Liquid crystal dimers
Nematic liquid crystals
4-Nitrostilbene
Isomerism

ABSTRACT

A new liquid crystal dimer, 1,12-*bis*(4-(2-(4-nitrophenyl)ethenyl)phenoxy)dodecane, was synthesized and structurally characterized. The compound exhibited enantiotropic nematic phase. The spectroscopic properties were analysed by UV–Vis and fluorescence techniques. Theoretical calculations were used to predict the UV–Vis spectral properties of three isomers and propose a mechanism of conversion between them. The obtained results present a solid basis for the future studies on the stilbene-based liquid crystal dimers, thus affording guidelines for development of a structure–property relationship of these compounds.

© 2021 Elsevier B.V. All rights reserved.

1. Introduction

Liquid crystal (LC) dimers contain two mesogenic units linked by a flexible spacer, usually an alkyl chain [1–3]. Anisotropic interactions between these units produce the LC functional assemblies, whereas the alkyl chain is responsible for additional fluidity and flexibility, thus enabling LC behaviour to be observed in wide temperature ranges. Different combinations of mesogenic units have given rise to materials exhibiting unusual behaviour [3]. This involves a significant dependence of their transitional features on the length and parity of the spacer, nematic–nematic transitions and alternating smectic phases [1]. The research in this field has been very dynamic, especially regarding their applications as dopants for LC display mixtures with faster relaxation times [4,5]. Several LC dimers have been found to exhibit a strong flexoelectric coupling [6,7].

Incorporation of selected mesogenic units with different properties into the molecular design of LC dimers allow formation of supramolecular architectures through interactions, which can be controlled by various external stimuli. Because of its luminescent properties and liquid crystallinity, a donor–π–acceptor system containing 4′-nitrostilbene unit is of particular interest in obtaining multi-functional materials [8,9]. Chen *et al.* applied external stimuli, including heat, mechanical force and ultrasound to the LC state of 4-alkoxy-4′-nitrostilbenes at supercooled temperatures to trigger different crystallization processes, which result in polymorphs with various luminescent properties [10]. Furthermore, polymeric films with different degrees of cross-linking were obtained by *in situ* photopolymerization of LCs based on alkoxynitrostilbenes [11]. Wu and co-workers prepared LCs with anisotropic fluorescence emission by ionic self-assembly from a copolymer and oppositely charged fluorescent rod-like dye containing this scaffold [12]. A series of bent-core molecules bearing 4-nitrostilbene in a side wing was also reported [13]. In this case, relatively small modifications in their structure significantly influenced the supramolecular assembly, which was further reflected in formation of various LC phases.

We aim to explore the effectiveness of the 4-nitrostilbene unit in promoting LC behaviour in dimers. To the best of our knowledge, only a non-symmetric LC dimer composed of the azobenzene and nitrostilbene units has been reported so far [14]. This compound has a nematic phase and is sensitive to the light from the UV and visible range and exhibits luminescence in the visible area. We expect that these functional π-conjugated systems become promising candidates for advanced technological applications.

* Corresponding author.
E-mail address: ntrisovic@tmf.bg.ac.rs (N. Trišović).

https://doi.org/10.1016/j.molliq.2021.116969
0167-7322/© 2021 Elsevier B.V. All rights reserved.

2. Material and methods

All starting materials, reagents and solvents were obtained from commercial suppliers and used without further purification. The synthetic route to the investigated LC dimer is presented in Scheme 1. 4-Hydroxy-4′-nitrostilbene was prepared according to a procedure from the literature [15]. Because the characterization data of this compound are in agreement with those previously reported, experimental details are not included here.

The FTIR spectrum of the synthesized compound was recorded with a Bomem MB series 100 spectrophotometer in the ATR mode. The NMR spectral measurements were performed on a Bruker 300 spectrometer at 400 MHz for the ^{1}H NMR and 100 MHz for the ^{13}C NMR spectra. The spectra were recorded at room temperature in $CDCl_3$ using TMS as the internal standard. The elemental analysis of the synthesized compound was carried out by standard analytical micromethods using an Elemental Vario EL III microanalyzer. Its results were found to be in good agreement (±0.3%) with the calculated values.

The UV–Vis spectrum was recorded using spectroscopy grade DMF at $5{\cdot}10^{-6}$ and $1{\cdot}10^{-3}$ mol dm^{-3} concentrations, with an Ocean Optics QE65 Pro spectrometer with tungsten and halogen lamps. Photoluminescence emission spectra were recorded by a Horiba Nanolog spectrofluorimeter, with 384 nm excitation and a 405 nm longpass filter.

The POM textures of the compound were investigated using Zeiss Axio Imager A1 polarizing microscope by placing LC sandwich cells with weak planar anchoring (achieved by unidirectionally rubbed glass plates) in an Instec heat stage. The POM textures were studied in an extremely slow heating–cooling cycle at ~ ±0.1 °C /min rate. DSC was performed using a TA Q20. The samples were obtained directly from recrystallization and measured at 5 °C/min heating and cooling rates.

2.1. Synthesis of 1,12-bis(4-(2-(4-nitrophenyl)ethenyl) phenoxy)dodecane

4-Hydroxy-4′-nitrostilbene (0.48 g, 2.0 mmol) was dissolved in DMF (30 mL) and potassium carbonate (1.38 g, 10 mmol) was added. After 30 min of stirring, 1,12-dibromododecane (0.32 mg, 0.98 mmol) was added and after 18 h of stirring at room temperature, the reaction mixture is poured into water (150 mL). The precipitate formed was filtered and recrystallized from DMF to give yellow solid. Yield: 38%. FTIR (ATR) υ 2920, 2850, 1587, 1572, 1505, 1473, 1334, 1323, 1269, 1246, 1173, 1108, 1033, 1004, 975, 952, 875, 841, 749, 716, 686, 630, 582, 530, 452 cm^{-1}; ^{1}H NMR ($CDCl_3$) δ [ppm]: 1.26–1.39 (m, 12H, –CH_2–), 1.44–1.51 (m, 4H, –CH_2–), 1.81 (quin, 4H, *J* = 7.1 Hz, –CH_2–), 3.99 (t, 4H, *J* = 6.6 Hz, –CH_2O–), 6.92 (d, 4H, *J* = 8.8 Hz, –C_6H_4–), 7.0 (d, 2H, *J* = 16.4 Hz, –CH = CH–), 7.23 (d, 2H, *J* = 16.4 Hz, –CH = CH–) 7.49 (d, 4H, *J* = 8.8 Hz, –C_6H_4–), 7.60 (d, 4H, *J* = 8.8 Hz, –C_6H_4–), 8.21 (d, 4H, *J* = 8.8 Hz, –C_6H_4–). ^{13}C NMR ($CDCl_3$) δ [ppm]: 26.0, 29.2, 29.4, 29.5, 68.1, 114.9, 123.9, 124.2, 126.5, 128.4, 128.8, 133.0, 144.3, 146.4, 159.9; elemental analysis calcd [%] for $C_{40}H_{44}N_2O_6$: C 74.05, H 6.84, N 4.32; found: C 74.08, H 6.80 N, 4.38.

2.2. Quantum chemical calculations

The calculations were performed using the Gaussian09 program package [16]. Three compound isomers were optimized by using the B3LYP functional, 6-31G(d,p) basis set and SMD solvation model for DMF solvent. Molecular Electrostatic Potential Surface (MEPS) calculations were performed at same level of theory. Time dependent density functional theory (TD-DFT) was employed to compute the UV–Vis spectra. For these calculations, a benchmark study was performed using BMK and CAM-B3LYP functionals, 6-31G(d,p) and def2-TZVP basis sets, and PCM and SMD solvation models for DMF solvent.

The prediction of the conversion mechanism between three isomer forms were performed at B3LYP/6-31G(d,p) level of theory. The general protocol used for investigation of mechanisms was as follows: obtaining the structure of the transition state (using TS calculations), and verifying the truthfulness of the TS by IRC (intrinsic reaction coordinate) calculations. IRC calculations also provided the reaction path, followed in two directions from the transition structure to the equilibrium geometries of reactants and products.

3. Results and discussion

A symmetric LC dimer where two 4-nitrostilbene units are connected with a dodecamethylene spacer *via* ether linkages, 1,12-*bis*(4-(2-(4-nitrophenyl)ethenyl)phenoxy)dodecane, was synthesized and characterized here. The synthetic route for the preparation of this compound involved a condensation reaction between 4-nitrophenylacetic acid and 4-hydroxybenzaldehyde giving 4-hydroxy-4′-nitrostilbene and its reaction with 1,12-dibromododecane in the presence of K_2CO_3 (Scheme 1).

The investigated compound is an enantiotropic LC (Fig. 1**a–1e**), which exhibits a conventional nematic phase in a temperature range of 20 and 30 °C on heating and cooling, respectively (Fig. 1). Attard and co-workers reported a structurally-related LC dimer consisting of two 4-nitroazobenzene units and the same spacer (**Fig. S4**, Supplementary data, [17]). This compound also enantiotropically exhibited a nematic phase, but its clearing point was lower for 20 °C. A LC dimer having the 4-(4-nitrobenzoyloxy) phenoxy group as two identical mesogenic terminal units connected *via* dodecamethylene spacer, however, formed a monotropic smectic phase in a narrow temperature range, as reported by Jin *et al.* (**Fig. S4**, Supplementary data, [18]). Evidently, such a trend implies that the charge transfer interaction between two 4-nitrostilbene units is greater than between two 4-nitroazobenzene or 4-(4-nitrobenzoyloxy)phenyl units [3]. Fig. 1**f** presents the potential surface in the molecule affecting the meso-

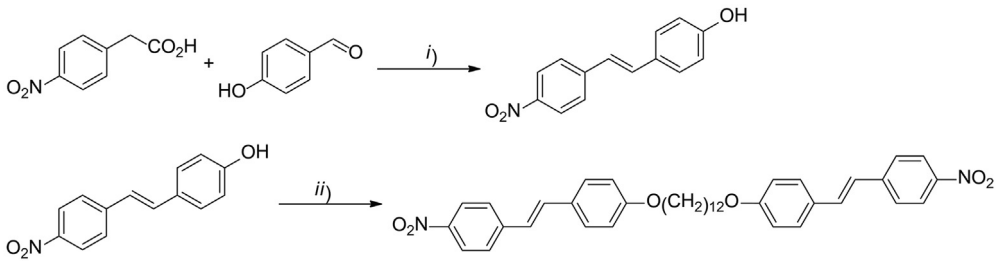

Scheme 1. Synthesis of 1,12-*bis*(4-(2-(4-nitrophenyl)ethenyl)phenoxy)dodecane. Reagents and conditions: *i*) piperidine, 110 °C, 6 h; *ii*) 1,12-dibromododecane, K_2CO_3, DMF, rt, 18 h.

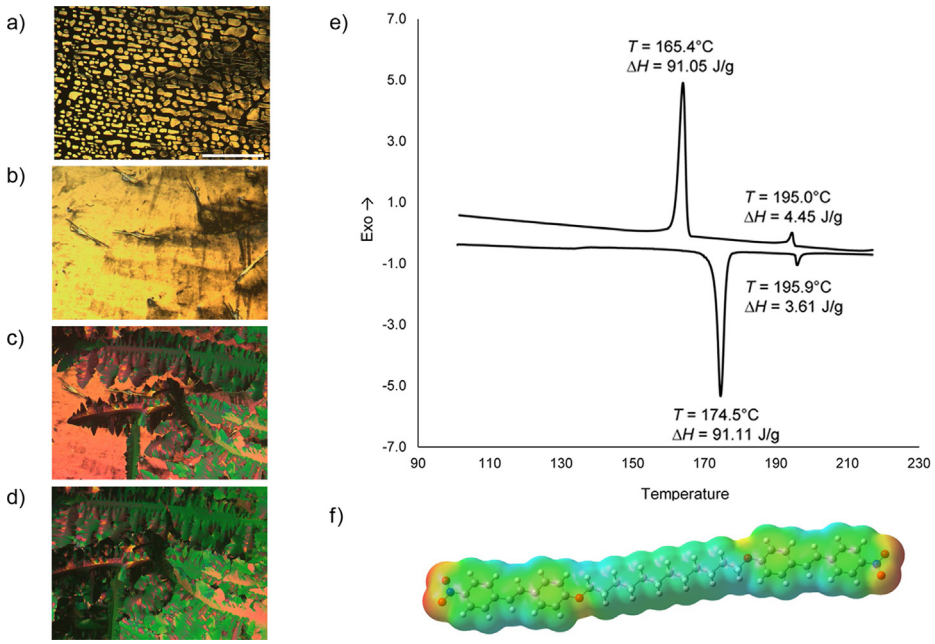

Fig. 1. Polarizing optical microscope textures under crossed polarizers on cooling at a) 199.2 °C (isotropic-to-nematic phase transition), b) 198.5 °C, c) 167.2 °C and d) 87.0 °C. The scale bar in a) denotes 300 μm. e) Results of differential scanning calorimetry during the second heating and cooling. f) Molecular electronic potential surface of the investigated compound (both double bonds being *trans*). Red areas indicate an increase in the electron density, while positive ones are represented by the blue regions.

gen interactions. The map shows that the most negative potential (red color) occurs above the O atom of the nitro group. Neutral potentials (green color) appear above the aromatic rings. The middle part of the molecule, above the aliphatic chain, as well as, the part above the C–H groups of the aromatic rings, represent a region with a positive potential (blue color). As there are no classical hydrogen bonding donors in the molecule, it can be expected that interactions of the aromatic fragments give the highest contribution to the stability. In addition, interactions between the aliphatic and aromatic fragments should also make a significant contribution to the stability, due to the large contribution of electrostatic interactions between them.

The absorption and emission spectrum of the investigated LC dimer in DMF are presented in Fig. 2 at two different concentrations. DMF is chosen, because the investigated compound is insoluble in most commonly used organic solvents. The absorption spectrum consists of an intense band at 383 nm, while a lower intensity band emerges approximately at 265 nm and overlap with the solvent cutoff. The emission spectrum is broad and structureless with the maximum at around 600 nm (independent of the concentration). A smaller peak originating from the C–H Raman mode from the solvent is also observed at around 432 nm.

The detailed photoluminescence map, taken in 2 nm steps for both excitation (EX) and emission (EM), is given in **Fig. S5** for the higher concentration (Supplementary data).

Theoretical calculations performed using Gaussian 09 program package [16] enabled us to analyse the UV–Vis spectral properties of the compound isomers and to propose a mechanism of conversion between them. Depending on the configuration around two double bonds within 4-nitrostilbene units, this compound can exist in three forms: *trans–trans*, *trans–cis*, and *cis-cis* forms (Fig. 3**a**). The structures of all three possible isomers were theoretically predicted at B3LYP/6-31G(d,p) level of theory and SMD solvation model. Because the studied molecule is quite large, some computational compromise had to be made. To achieve a balance between the computational precision and cost, optimizations were performed using the typical hybrid B3LYP functional, while a smaller 6-31G(d,p) basis set was used for all the atoms. To improve accuracy of calculations, the tight convergence criteria was used. Based on the energies of the optimized structures, it was shown that the *trans–trans* isomer is the most stable (Fig. 3**a**). The *trans–cis* isomer is less stable for 6.7 kcal/mol than the *trans–trans* isomer, while the *cis–cis* isomer is less stable for about 13.5 kcal/mol. Although the *trans* C = C bond is more stable for steric reasons, the formation of intramolecular C–H···π interaction between two phenyl rings

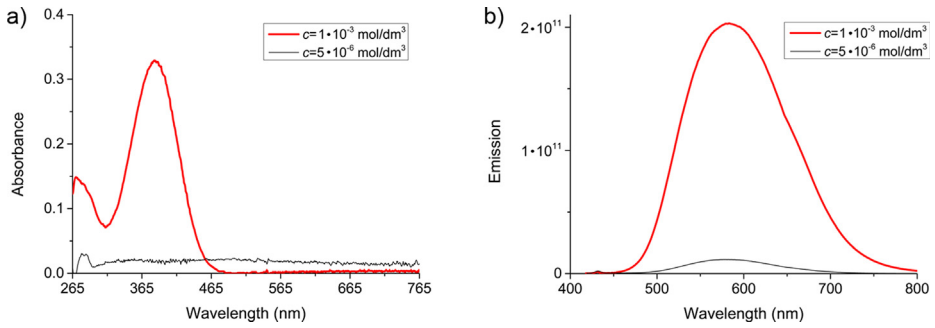

Fig. 2. a) The absorption and b) emission spectrum of the investigated LC dimer (excitation at 384 nm) in DMF.

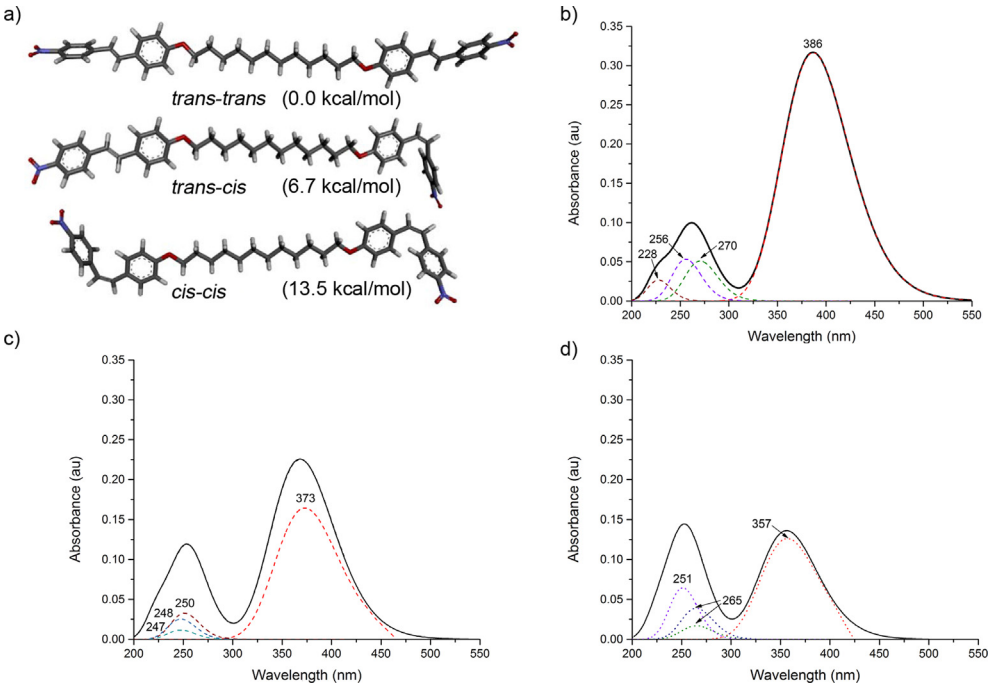

Fig. 3. a) The optimized structures of three isomer forms of the studied compound. Theoretical UV–Vis spectrum for b) *trans–trans*, c) *trans–cis*, and d) *cis-cis*. (Solid line – simulated UV–Vis spectrum by Gaussian band shape, dashed lines – the individual electronic transitions).

is a reason for the slight differences in the isomer energies. Regarding that the *trans–trans* isomer is the most stable one, one can expect that it is the most abundant in the solid state.

For the theoretical UV–Vis spectrum, a benchmark study (**Table S1**) was performed on the optimized structure having both double bonds in *trans* configuration (*trans–trans* isomer), by changing the methods (BMK and CAM-B3LYP), basis sets (6-31G(d,p) and def2-TZVP), and solvation model (PCM and SMD). The results of the benchmark study showed that the theoretical UV–Vis spectrum of *trans–trans* isomer, obtained by using of CAM-B3LYP/6-31G(d,p)/SMD approach, match very well with the experimental results (Fig. 3**b** and Fig. 2**a**). Additionally, the theoretical UV–Vis spectra for *trans–cis* and *cis-cis* isomers were also calculated (Fig. 3**c and d**).

Considering the positions and intensities of the calculated spectra, it can be concluded that the calculated spectrum of *trans–trans* isomer best corresponds to the experimental spectrum of the studied compound. The experimental peaks (383 nm, Fig. 2**a**) for the more intense and lower intense band (approx. 265 nm) are in a very good agreement with the UV–Vis maxima of *trans–trans* isomer (386 nm and 263 nm, Fig. 3**b**). Compared to the most intense band of the *trans–trans* isomer (λ = 386 nm and f = 2.347), the band of *trans–cis* isomer has the lower intensity (f = 1.220) and it is shifted to lower wavelengths (λ = 373 nm). On the other hand, the lower intensity band is also shifted to lower wavelengths (maximum at 250 nm) (Fig. 3**c**). The most intense band of the *cis-cis* isomer is shifted even more toward lower wavelengths (λ = 357 nm), and with an even more pronounced fall in intensity (f = 0.936). In contrast to other two isomers, the peak at about 250 nm is (slightly) higher in intensity than the peak at a longer wavelength (Fig. 3**d**).

The position, intensity and nature of the most intense transitions observed in the theoretical spectra of all three isomers are given in Table 1. The strong absorption band reflects the transition at approx. 350–380 nm. In a case of *trans–trans* and *cis-cis* isomer, HOMO, HOMO-1, LUMO and LUMO + 1 are major molecular orbitals (MO) contributors to this transition. The major MO contributors to the most intense band of *trans–cis* isomer derived from HOMO and LUMO orbitals. HOMO, HOMO-n, LUMO, and LUMO-n (n = 1, 2, 3, 4, 5) orbitals participate in electronic transitions at lower wavelengths (**Fig. S6, S7 and S8**).

The prediction of mechanism of conversion from the most stable (*trans–trans*) isomer to the most unstable (*cis-cis*) isomer (Fig. 4) was performed at B3LYP/6-31G(d,p) level of theory. Calculations reveal that the transition is not direct, but goes over *trans–cis* form and states known as saddle points (SP).

There are two saddle points (Fig. 4**b and c**), and they represent carbenes, species that contain a neutral carbon atom with a valence of two and two unshared valence electrons (singlet state). The carbenes are formed by the transition of the H atom from one of the C atoms of the double bond to another C atom of this bond. The saddle points only differ in configuration around the double bond. Namely, the SP1 carbene possesses the C = C bond with *trans* configuration (Fig. 4**b**), while SP2 carbene has the *cis* double bond (Fig. 4**c**).

The conversion from the *trans–trans* to the *trans–cis* isomer requires the energy of about 83.1 kcal/mol (the first activation energy, Fig. 4**a**). This means that the compound should be irradiated with light of λ = 344 nm to achieve the first transition state (TS1), which, after relaxation, passes to the first saddle point (SP1). The entire path includes four transition states, structures of which are shown in Fig. 4**b and c**. On the potential energy path, energy barriers between the saddle points (SP1 and SP2) and the corresponding minima are 5.6 and 3.3 kcal/mol, respectively, thus indicating the similar tendencies towards the adjacent minima. The transition from the *trans–cis* to the *cis-cis* isomer also requires the energy of about 83.1 kcal/mol, (the second activation energy, Fig. 4**a**).

Based on the proposed mechanism of conversion (Fig. 4**a**), it is clear that the *trans–trans* isomer, by irradiation, transforms into a carbene with the structure designated as SP1. This carbene is in the shallow minimum, with a similar sizes of reaction barriers for transition to the *trans–trans* or *trans–cis* isomer (barriers are about 4.7 and 5.6 kcal/mol). After termination of irradiation, it

Table 1
The position (λ, in nm), intensity (f) and nature of the most intense transitions, observed in the theoretical spectra of all three isomers.

λ	*f*	Major MO contributors		
trans–trans				
386	2.347	H-1 → LUMO (42%)	HOMO → L + 1 (42%)	
270	0.379	H-1 → L + 3 (32%)	HOMO → L + 2 (32%)	
256	0.396	H-3 → L + 1 (17%)	H-2 → LUMO (18%)	H-1 → L + 3 (11%)
228	0.199	H-5 → L + 1 (34%)	HOMO → L + 6 (22%)	H-4 → LUMO (16%)
trans–cis				
373	1.220	HOMO → LUMO (88%)		
250	0.243	H-1 → L + 3 (69%)		
248	0.189	H-3 → LUMO (52%)	HOMO → L + 2 (20%)	HOMO → LUMO (10%)
247	0.088	H-1 → L + 7 (25%)	H-4 → L + 1 (16%)	H-1 → L + 4 (14%)
cis-cis				
357	0.936	HOMO → L + 1 (42%)	H-1 → LUMO (38%)	
265	0.125	H-2 → LUMO (64%)	H-4 → LUMO (10%)	
265	0.289	H-3 → L + 1 (64%)	H-5 → L + 1 (10%)	
251	0.478	H-1 → L + 3 (30%)	HOMO → L + 2 (39%)	

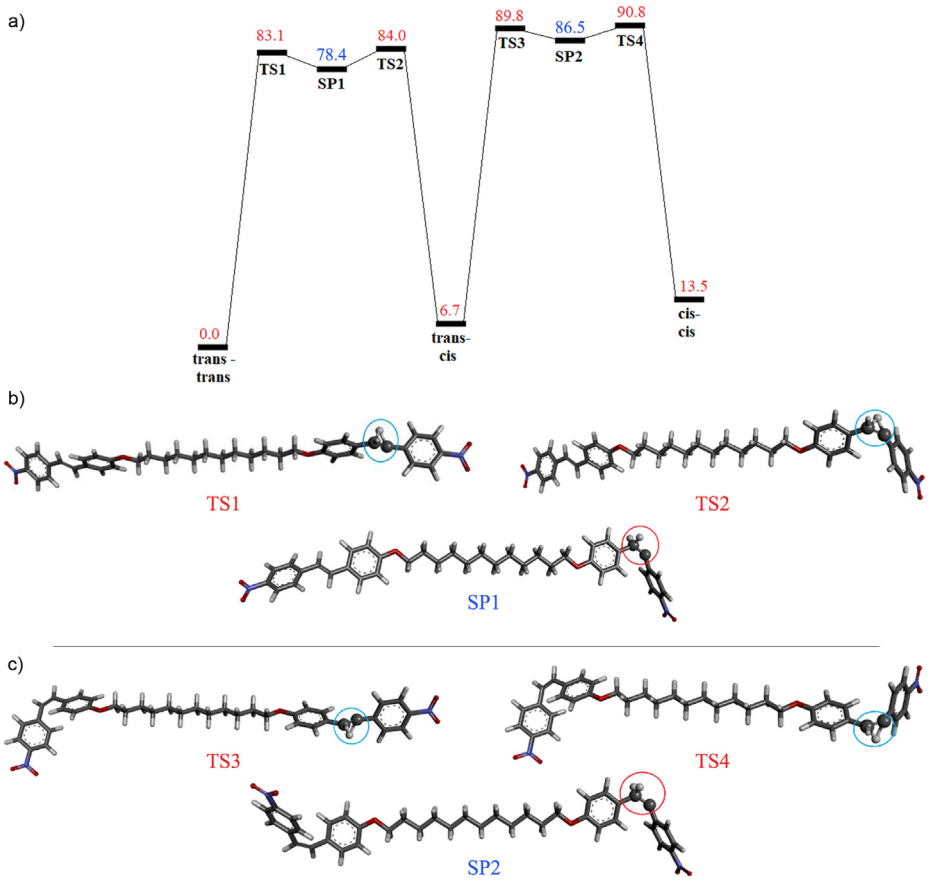

Fig. 4. a) The mechanism of conversation of *trans–trans* form to *cis-cis* isomer of the studied compound. b) The optimized structures of transition states (TS) and two carbenes, which represent the saddle points (SP) in the predicted mechanism of conversion.

can be expected that a certain amount of the SP1 carbene will pass into the *trans–cis* isomer, since the *trans–trans* isomer is more stable.

A large change in the dipole moments accompany the conversion between the isomers. The dipole moment components (μ_x, μ_y, μ_z) and modulus (μ) for all three isomers are given in Table S2 in Supplementary data. As expected, the *trans–trans* and *cis-cis* isomers have zero dipole moment for symmetrical reasons. On the other side, the *trans–cis* isomer exhibits an overall dipole moment of 10 D, whereas μ_y yields the major contribution.

4. Conclusions

Having in mind advantageous features of LC dimers and the ever growing field of their applications, new, multifunctional ones are much needed. A new LC dimer, 1,12-*bis*(4-(2-(4-nitrophenyl)ethenyl)phenoxy)dodecane, exhibited enantiotropic nematic phase. A theoretical analysis of this molecule containing two identical isomerisable units showed that the *trans–cis* and *cis–cis* isomers are less stable than the *trans–trans* isomer for 6.7 and 13.5 kcal/mol, respectively. This also suggested the domination of *trans–trans* iso-

mer in the crystalline and nematic phases. Our findings further demonstrated that the mechanism of conversion of the most stable (*trans–trans*) form to the most unstable one (*cis-cis*) is not direct, but goes through the *trans–cis* form and two saddle points being carbene-type species. Overall, the obtained results not only identify the 4-nitrostilbene unit as a promising scaffold in design of LC dimers, but also extends our understanding of the isomerisation mechanism underlying their photophysical features.

Finally, for practical applications, we note the importance of eventual changes of physical parameters (such as electric conductivity, or dielectric constant [19,20]) *via* isomerization upon illumination, measurements that are planned for the future.

CRediT authorship contribution statement

Kristina Gak Simić: Investigation, Formal analysis, Validation, Writing - original draft. **Ivana Đorđević:** Investigation, Formal analysis, Software, Data curation, Visualization. **Goran Janjić:** Resources, Formal analysis, Software, Data curation, Writing - review & editing. **Dániel Datz:** Investigation, Formal analysis, Resources. **Tibor Tóth-Katona:** Investigation, Formal analysis, Resources. **Nemanja Trišović:** Conceptualization, Supervision, Resources, Writing - review & editing.

Declaration of Competing Interest

The authors declare that they have no known competing financial interests or personal relationships that could have appeared to influence the work reported in this paper.

Acknowledgement

This work was supported by the Ministry of Education, Science and Technological Development of the Republic of Serbia (Contract No. 451-03-9/2021-14/200135; 451-03-9/2021-14/200287, 451-03-9/2021-14/200026). T.T.-K. acknowledges the financial support from the National Research, Development and Innovation Office (NKFIH) grant no. FK 125134.

Appendix A. Supplementary material

Supplementary data to this article can be found online at https://doi.org/10.1016/j.molliq.2021.116969.

References

[1] C.T. Imrie, P.A. Henderson, Liquid crystal dimers and higher oligomers: between monomers and polymers, Chem. Soc. Rev. 36 (2007) 2096–2124, https://doi.org/10.1039/b714102e.
[2] E. Forsyth, D.A. Paterson, E. Cruickshank, G.J. Strachan, E. Gorecka, R. Walker, J. M.D. Storey, C.T. Imrie, Liquid crystal dimers and the twist-bend nematic phase: on the role of spacers and terminal alkyl chains, J. Mol. Liq. 320 (2020) 114391, https://doi.org/10.1016/j.molliq.2020.114391.
[3] C.T. Imrie, Non-symmetric liquid crystal dimers: how to make molecules intercalate, Liq. Cryst. 33 (11-12) (2006) 1449–1485, https://doi.org/10.1080/02678290601140498.
[4] K. Araya, D.A. Dunmur, M.C. Grossel, G.R. Luckhurst, S.E. Marchant-Lane, A. Sugimura, Flexible dimers as dopants for liquid crystal display mixtures with faster relaxation times, J. Mater. Chem. 16 (2006) 4675–4689, https://doi.org/10.1039/B610598J.
[5] M. Tokita, M. Itoh, K. Marumo, Y. Harada, S. Kang, K. Sakajiri, J. Watanabe, Macrocyclised pheynyl cinnamate dimer utilisable as photoresponsive chiral dopant for nematic liquid crystals, Liq. Cryst. 40 (7) (2013) 900–905, https://doi.org/10.1080/02678292.2013.790094.
[6] A. Varanytsia, L.-C. Chien, Giant flexoelectro-optic effect with liquid crystal dimer CB7CB, Sci. Rep. 7 (2017) 41333, https://doi.org/10.1038/srep41333.
[7] A. Ferrarini, C. Greco, G.R. Luckhurst, On the flexoelectric coefficients of liquid crystal monomers and dimers: a computational methodology bridging length-scales, J. Mater. Chem. 17 (2007) 1039–1042, https://doi.org/10.1039/B618928H.
[8] S. Bollo, E. Soto-Bustamante, L.J. Núñez-Vergara, J.A. Squella, Electrochemical study of nitrostilbene derivatives: nitro group as a probe of the push–pull effect, J. Electroanal. Chem. 492 (1) (2000) 54–62, https://doi.org/10.1016/S0022-0728(00)00265-5.
[9] C.-C. Chen, T. Hinoue, I. Hisaki, M. Miyata, N. Tohnai, A tunable photoluminescence system consisting of liquid-crystalline trans-alkoxy-nitrostilbenes with n-alkyl chains, Tetrahedron Lett. 54 (13) (2013) 1649–1653, https://doi.org/10.1016/j.tetlet.2013.01.013.
[10] C.-C. Chen, T. Hinoue, J.-H. Liu, I. Hisaki, M. Miyata, N. Tohnai, Solid-state photoluminescence modulation of trans-alkoxy-nitrostilbene dyes by triggering the solidification of mesophases via external stimuli, Bull. Chem. Soc. Jpn. 87 (1) (2014) 76–87, https://doi.org/10.1246/bcsj.20130262.
[11] C. Sánchez, B. Villacampa, R. Alcalá, C. Martínez, L. Oriol, M. Piñol, J.L. Serrano, Mesomorphic and orientational study of materials processed by in situ photopolymerization of reactive liquid crystals, Chem. Mater. 11 (10) (1999) 2804–2812, https://doi.org/10.1021/cm991036x.
[12] J. Wu, Z. Yi, X. Lu, S. Chen, Q. Lu, Formation and properties of liquid crystalline supramolecules with anisotropic fluorescence emission, Polym. Chem. 5 (2014) 2567–2573, https://doi.org/10.1039/C3PY01544K.
[13] N. Trišović, L. Matović, T. Tóth-Katona, R. Saha, A. Jákli, Mesomorphism of novel stilbene-based bent-core liquid crystals, Liq. Cryst. 48 (7) (2021) 1054–1064, https://doi.org/10.1080/02678292.2020.1839800.
[14] I. Korbecka, J. Jaworska, Z. Galewski, Novel fluorescent liquid crystal containing azobenzene and stilbene moieties-synthesis, mesogenic and spectroscopic studies, Dye. Pigment. 140 (2017) 166–168, https://doi.org/10.1016/j.dyepig.2016.11.059.
[15] V.R. Vangala, B.R. Bhogala, A. Dey, G.R. Desiraju, C.K. Broder, P.S. Smith, R. Mondal, J.A.K. Howard, C.C. Wilson, Correspondence between molecular functionali-ty and crystal structures. Supramolecular chemistry of a family of homologated aminophenols, J. Am. Chem. Soc. 125 (47) (2003) 14495–14509, https://doi.org/10.1021/ja037227p.
[16] M.J. Frisch, G.W. Trucks, H.B. Schlegel, G.E. Scuseria, M.A. Robb, J.R. Cheeseman, G. Scalmani, V. Barone, G.A. Petersson, H. Nakatsuji, X. Li, M. Caricato, A. Marenich, J. Bloino, B.G. Janesko, R. Gomperts, B. Mennucci, H.P. Hratchian, J.V. Ortiz, A.F. Izmaylov, J.L. Sonnenberg, D. Williams-Young, F. Ding, F. Lipparini, F. Egidi, J. Goings, B. Peng, A. Petrone, T. Henderson, D. Ranasinghe, V.G. Zakrzewski, J. Gao, N. Rega, G. Zheng, W. Liang, M. Hada, M. Ehara, K. Toyota, R. Fukuda, J. Hasegawa, M. Ishida, T. Nakajima, Y. Honda, O. Kitao, H. Nakai, T. Vreven, K. Throssell, J.A. Montgomery Jr., J.E. Peralta, F. Ogliaro, M. Bearpark, J.J. Heyd, E. Brothers, K.N. Kudin, V.N. Staroverov, T. Keith, R. Kobayashi, J. Normand, K. Raghavachari, A. Rendell, J.C. Burant, S.S. Iyengar, J. Tomasi, M. Cossi, J.M. Millam, M. Klene, C. Adamo, R. Cammi, J.W. Ochterski, R. L. Martin, K. Morokuma, O. Farkas, J.B. Foresman, D.J. Fox, Gaussian 09, Gaussian Inc, Wallingford CT, 2009.
[17] G.S. Attard, S. Garnett, C.G. Hickman, C.T. Imrie, L. Taylor, Asymmetric dimeric liquid crystals with charge transfer groups, Liq. Cryst. 7 (4) (1990) 495–508, https://doi.org/10.1080/02678299008033826.
[18] J.-I. Jin, J.-S. Kang, B.-W. Jo, R.W. Lenz, Synthesis and properties of thermotropic compounds with two terminal mesogenic units and a central spacer III. Homologous series of α, ω-bis[4-(p-nitrobenzoyloxy)phenoxy]alkanes, Bull. Korean. Chem. Soc. 4 (1983) 176–180.
[19] H. Jing, M. Xu, Y. Xiang, E. Wang, D. Liu, A. Poryvai, M. Kohout, N. Éber, Á. Buka, Light tunable gratings based on flexoelectric effect in photoresponsive bent-core nematics, Adv. Optical Mater. 7 (8) (2019) 1801790, https://doi.org/10.1002/adom.v7.810.1002/adom.201801790.
[20] N. Begum, S. Kaur, Y. Xiang, H. Yin, G. Mohiuddin, N.V.S. Rao, S. Kumar Pal, Photoswitchable bent-core nematic liquid crystals with methylated azobenzene wing exhibiting optic-field-enhanced Freedericksz transition effect, J. Phys. Chem. C 124 (2020) 874–885, https://doi.org/10.1021/acs.jpcc.9b09326.